Mechanical Properties of Axons

Roberto Bernal,[1] Pramod A. Pullarkat,[2] and Francisco Melo[1]
[1]*Departamento de Física, Universidad de Santiago de Chile, and CIMAT, Avenida Ecuador 3493, Casilla 307, Correo 2, Santiago, Chile*
[2]*Experimentalphysik I, University of Bayreuth, D95440 Bayreuth, Germany*
(Received 26 January 2007; published 3 July 2007)

The mechanical response of PC12 neurites under tension is investigated using a microneedle technique. Elastic response, viscoelastic relaxation, and active contraction are observed. The mechanical model proposed by Dennerll *et al.* [J. Cell Biol. **109**, 3073 (1989).], which involves three mechanical devices—a stiff spring κ coupled with a Voigt element that includes a less stiff spring k and a dashpot γ—has been improved by adding a new element to describe the main features of the contraction of axons. This element, which represents the action of molecular motors, acts in parallel with viscous forces defining a global tension response of axons T against elongation rates $\dot{\delta}_k$. Under certain conditions, axons show a transition from a viscoelastic elongation to active contraction, suggesting the presence of a negative elongation rate sensitivity in the curve T vs $\dot{\delta}_k$.

DOI: 10.1103/PhysRevLett.99.018301 PACS numbers: 83.80.Lz, 83.60.−a, 87.19.La

The cytoskeleton—a crosslinked biopolymer network—provides mechanical strength to the cell and also drives vital functions such as locomotion, division, and intracellular transport [1]. These remarkable properties arise from the ability of the filaments to reorganize through a polymerization-depolymerization process and through the action of molecular motors that generate forces and motion using chemical energy [1]. Thus, the cytoskeleton is a complex ''active gel'' with fascinating properties. In recent years, the advent of novel techniques has allowed progress in our understanding of live cell mechanics [2–5]. However, modeling cytoskeletal mechanics at the level of a cell is hindered by cellular heterogeneity and the complex interaction of the cell with the extracellular matrix.

In contrast to most cells, axons can be approximated as a uniform, uniaxial structure containing all the main ingredients of the cell cytoskeleton. Typically, the axonal cytoskeleton is made up of a cortex of actin filaments attached to the plasma membrane, a core of neurofilaments, and aligned and bundled microtubules [1]. As in other cells, and as our results will demonstrate, molecular motors provide the axon with the ability to generate active contractile stresses [6]. The active as well as viscoelastic properties of axons are expected to be important physiologically in axonal retraction after injury or during rewiring [6], and in stretching during limb movement [7].

Using PC12 neurites as a model system for axons [8,9], we perform a systematic investigation of their mechanical response. We employ an axon-pulling setup and a microneedle to achieve accurate determination of force and strain of axons. We present measurements of the elastic response and viscous dissipation in axons. Furthermore, we characterize the active tension in axons and a transition from a passive viscoelastic relaxation to an active contraction. We model our data using a novel mechanical representation for the molecular motors, introducing a minimal set of experimentally validated components. The transition from viscous elongation to active contraction is described in the framework of a negative strain rate sensitivity.

PC12 cells were grown on collagen-coated coverslides using standard techniques [9]. The cells were maintained at 37 °C and observations made using a Nikon Eclipse TE-300 microscope with a $40\times/0.6$ objective in phase contrast mode. Images were recorded using an analog CCD camera and a frame grabber card. Glass microneedles were fabricated using a pipette puller (Flaming/Brown P-87) and calibrated using a frequency response analysis. The stiffness constant was of the order of $k_n \sim 0.1$ mN/m. In order not to perturb the surrounding cells, we modified the needle to get an L-shaped (¬) tip. To apply a stretch [Fig. 1(a)], the midpoint of the neurite was displaced laterally by driving the sample chamber perpendicular to the length of the neurite using a precision dc motor (Thorlabs T25X-D/M). Only the cases where the adhesion points of the axon remained fixed during measurement were used. The force was inferred by measuring the tip deflection (Fig. 1).

The general mechanical response of the axon is complex and we aim at obtaining the maximum of experimental information to characterize it. Let us first consider the simplest situation in which the axon is modeled as an

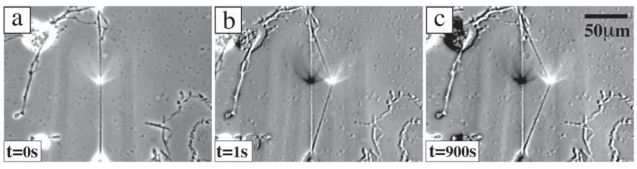

FIG. 1. (a) An axon with the needle in contact (bright spot). (b) Initial deformation caused by moving the motor at 25 μm/s for 1 s [with the negative of image (a) added as reference]. (c) Subsequent evolution of the axon needle.

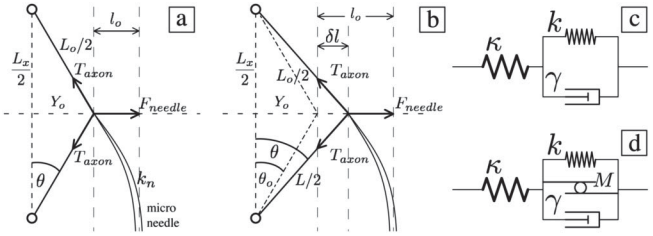

FIG. 2. (a) The axon and needle deflections and involved variables for an elastic deformation. (b) Variables for a viscoelastic mechanical response. (c) Classical model for axons proposed in Ref. [8]. (d) Model including motors action.

elastic rope of initial length L_x, subjected to a force applied at the middle point. Under this force, the middle point moves a distance Y_0 and the axon elongates by $\Delta L = L_0 - L_x$ as in Fig. 2(a). The needle force F_{needle} has a magnitude $k_n l_0$, where l_0 is the tip deflection. The equilibrium between F_{needle} and the axon tension T_{axon} is $F_{\text{needle}} = 2T_{\text{axon}} \sin\theta$. Thus, if the spring constant of the axon is κ, $T_{\text{axon}} = \kappa\delta_\kappa$, where δ_κ is the elastic elongation. However, the initial state of the axon is not known, since the length L_x is not necessarily the length at which the axon is under zero tension. Indeed, even in the absence of a lateral force, due to the action of molecular motors, the axon might sustain an initial tension T_0 [6,10,11] that must be included for a consistent analysis. Thus, $F_{\text{needle}} = 2(\kappa\delta_\kappa + T_0) \times \sin\theta$. From Fig. 2(a), we observe that $\sin\theta = 2Y_0/L_0$ and using the approximation $\sin\theta \ll 1$, the equilibrium becomes [12],

$$F_{\text{needle}} \approx \kappa \frac{L_x}{2}\theta^3 + 2T_0\theta. \quad (1)$$

Real axons are viscoelastic structures. However, Eq. (1) holds for sufficiently fast deformations, for which viscous effects can be neglected [11]. This was accomplished by imposing a high, constant speed to the motor for a short time. Since the viscoelastic relaxation times are larger than 10 s [see Fig. 4(a)], the elastic response was captured for deformations performed over less than 1 s. As seen in Fig. 3(a), this response agrees well with the pure-elastic response approximation. The parameter κ obtained from the interpolation of the experimental data is displayed as a function of the ratio of the axon cross section to the initial axon length A/L_x in Fig. 3(b).

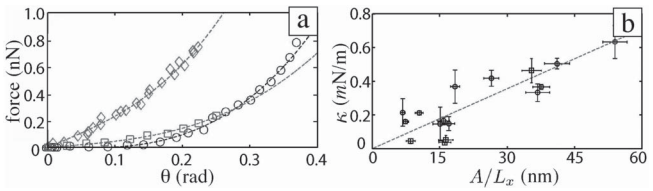

FIG. 3. (a) Force experienced by different axons as a function of θ during deformations at 25 μm/s for 1 s. The slope at $\theta = 0$ relates to T_0 and the nonlinear term in θ to κ. (b) κ for different neurites shows a roughly linear trend with A/L_x.

For a generic homogenous axon, the elastic constant κ is related to the ratio A/L_x and the Young's modulus E, as $\kappa = EA/L_x$. Despite dispersion from axon to axon, the data in Fig. 3(b) show a linear trend for κ vs A/L_x, which allows us to obtain an estimate for E averaged over many axons. In contrast, T_0 does not show any clear correlation with the axon geometry [11] (data not shown). Here, E is a composite modulus for the set of internal components like the cellular membrane, actin network, microtubules and protein crosslinkers. We obtain a value $E \simeq (12 \pm 2)$ k Pa which is comparable to the value obtained for living cells such as fibroblasts averaged over the whole cell [5]. This elastic modulus is much larger than the one reported for the growth cone [13] $E_{\text{gc}} \approx 100$ Pa, where the structure is almost completely free of microtubules and the actin filaments are very dynamic. The axon, on the other hand, is densely filled with microtubules.

In addition to the fast elastic response, pioneering experiments by Lamoureux *et al.* [10] and Dennerll *et al.* [8] have shown that axons exhibit a passive viscoelastic behavior. To account for the observed response, they proposed a simple mechanical model where the axon is approximated by a spring with constant κ in series with a combination of a spring k and a dashpot with friction

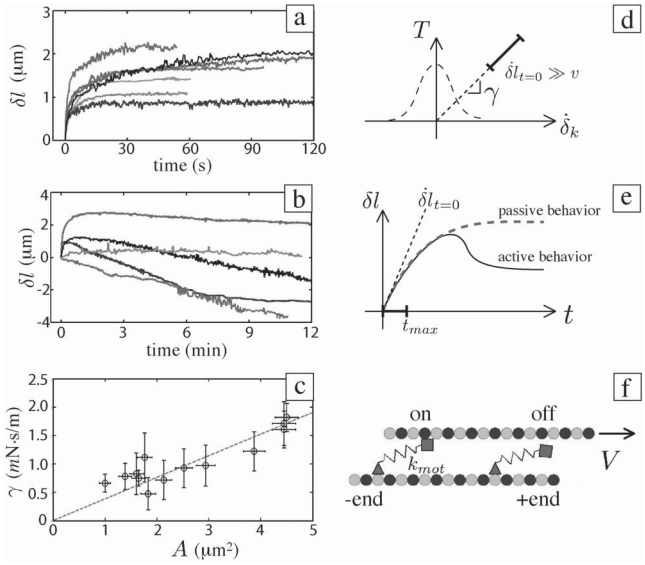

FIG. 4. (a) Viscoelastic relaxation that follows the initial elastic response in different neurites. The relaxation times are about 10 s. (b) Active behavior which results in a transition from a fast viscoelastic elongation to a slow contraction is observed in some cases. (c) γ as a function of cross-sectional area. (d) Schematic of the viscous and motor responses of an axon as a function of the $\dot{\delta}_k$. (e) In order to measure γ, $\dot{\delta}_k > v$. Thus, the initial slope of the δl-t curve depends only on γ and the external force. (f) The elastic energy stored in the spring k_{mot} is dissipated when motors detach from the filaments.

coefficient γ in parallel as in Fig. 2(c). These constants represent elastic interactions and dissipation between the different components within the axon. However, axonal contractions are often detected; i.e., there is an active behavior due to the molecular motors that this model does not include. Therefore, we propose adding a third element in parallel to k and γ. This new element, which we denote by M in Fig. 2(d), accounts for the average activity of the cytoskeletal motors within the axon. These three elements share a common elongation δ_k. We assume that the force f_M applied by element M is represented by a characteristic tension scale T_a and an arbitrary function of the ratio of deformation rate $\dot{\delta}_k$ to the characteristic speed v of molecular motors [14,15], i.e., $f_M = T_a f(\dot{\delta}_k/v)$. In general, this function decreases with $\dot{\delta}_k$ [16], vanishes at $\dot{\delta}_k/v > 1$, and has a maximum at null speed.

Mechanical balance is described by three equations, $2(\kappa\delta_\kappa + T_0)\sin\theta_0 = k_n(l_0 - \delta l)$ and $\kappa\delta_\kappa + T_0 = k\delta_k + \gamma\dot{\delta}_k + T_a f(\dot{\delta}_k/v)$, which represents force equilibrium of the element κ with both the microneedle and the combined element k-γ-M. In addition, the total elongation follows, $\delta_\kappa + \delta_k = \sin\theta_0\delta l + \delta_\kappa^o$, with $\delta_\kappa^o = k_n l_0/2\kappa\sin\theta_o - T_0/\kappa$ as the final elongation immediately after the initial elastic test. Note that here the initial length of the axon is L_0 instead of L_x, i.e., its length right after the fast elastic test [Fig. 2(b)]. Approximating θ by θ_0 and writing the elongations δ_κ, δ_k, and the elongation rate $\dot{\delta}_k$ as functions of δl, with $\alpha = \sin\theta_0$ and $\beta = (\alpha + k_n/2\alpha\kappa)$ leads to

$$\beta\gamma\dot{\delta}l + T_a f(\dot{\delta}_k/v) + k\left(\beta + \frac{k_n}{2\alpha k}\right)\delta l = \frac{k_n}{2\alpha}l_0, \qquad (2)$$

which forms the dynamical equation for the experimental analysis of the microneedle deflection.

Figure 4(a) shows the viscoelastic elongation of the axons observed immediately after the rapid elastic elongation. To measure γ, we take advantage of the fact that the force applied on the axon immediately after the elastic response is always greater than T_0. In other words, at early stages, the relaxation of the axon is assumed to be dominated by γ. This approximation holds if $\dot{\delta}_k/v > 1$, as shown in Fig. 4(d). Then Eq. (2) simplifies to $\beta\gamma\dot{\delta}l + k[\beta + (k_n/2\alpha k)]\delta l = (k_n/2\alpha)l_0$, with a solution $\delta l(t) = [k_n l_0/(2\alpha\beta k + k_n)][1 - \exp(-[(2\alpha\beta k + k_n)/2\alpha\beta\gamma]t)]$. Here, we determine the value of γ by taking only the initial experimental values from the deflection of the microneedle with an error less than 10%. The first term of the expansion is $k_n l_0/(2\alpha\beta\gamma)$ and from the experimental slope $\dot{\delta}l_0$ at early stages of the relaxation [Fig. 4(e)], we obtain $\gamma = (k_n l_0/2\alpha\beta\dot{\delta}l_0)$. Notice that the later stages of the relaxation may not necessarily be described by a linear dashpot. For instance, at elongation rates of the same order as v, the axon response is notably influenced by molecular motor action. Figure 4(c) shows a linear trend of γ with the cross-sectional area of the axon. From a physical point of view, this behavior can be captured with a simple model of viscosity as described by Howard [14]. Let us suppose that this dissipation arises from the friction between different filaments within the axon and the action of the molecular motors adhering to these filaments. Consider a molecular motor with the ability to adhere periodically to a filament as in Fig. 4(f). The adenosine-triphosphate (ATP) hydrolysis cycle time is τ and the constant of restitution for a motor is k_{mot}. The elongation that the motor undergoes by a displacement of the filament at speed V is $V\tau_{\mathrm{on}}$, where τ_{on} is the time that the motor remains adhered. The restitution force is $k_{\mathrm{mot}}V\tau_{\mathrm{on}}$. The elastic energy stored in k_{mot} is dissipated when the motor detaches from the filament. Then, the macroscopic drag coefficient γ is written in terms of the dissipation per motor in a cycle, that is to say, $\gamma \approx np\tau_{\mathrm{on}}k_{\mathrm{mot}}$, where $p = \tau_{\mathrm{on}}/\tau$ is the duty ratio of the motor and n is the number of motors per unit cross-sectional area A. Rewriting k_{mot} in terms of the ratio of Young's modulus to average length l_{mot} [14], that is characteristic for all protein motors, times A, leads to $\gamma \approx [p(E\hat{\tau}_{\mathrm{on}}/l_{\mathrm{mot}})]A$. Notice that $\hat{\tau}_{\mathrm{on}}$ characterize the average time that the motors remain attached during the hydrolysis cycle of ATP. To get some estimates, let us use the reasonable values of $l_{\mathrm{mot}} \approx 10$ nm as the typical length of a protein motor, $\delta \approx 5$ nm as the separation between monomers in the filament and $v \approx 1\ \mu$m/s as the typical motor velocity (see Table I). With this, we obtain a time scale for the attachment state $\hat{\tau}_{\mathrm{on}} \approx 5$ ms. From experiments, $A \approx 1\ \mu\mathrm{m}^2$, $E \approx 12$ kPa, and $\gamma \approx 0.6$ mN $\cdot$ s/m. Thus, we obtain $p \approx 0.1$, and $\hat{\tau} \approx \hat{\tau}_{\mathrm{on}}/p \approx 50$ ms as the average turnover cycle. These values depend on the concentration of molecular motors and ATP, and the type of organization of the motors. As a comparison, in fast muscle structures which involve myosin motors [14], these values are $\tau_{\mathrm{on}} \approx 1$ ms, $p \approx 0.14$, and a maximum value for $v \approx 5\ \mu$m/s.

In many cases, due to the action of the molecular motor, the viscoelastic relaxation is followed by a relatively slow contraction of the axon as in Fig. 4(b). Experiments on the force-velocity behavior of a collection of myosin molecular motors show a decrease in the velocity when the external force increases [15,17]. The functional dependence resembles a Gaussian [15]. We chose the macroscopic force averaged over the set of motors as a Gaussian func-

TABLE I. Comparison of values reported in Refs. [8,11] and the present Letter.

Model	L (μm)	κ (mN/m)	E (kPa)	k (mN/m)	γ (mM/m)	T_0 (nN)	T_a (nN)	v (μm/s)
Dennerll *et al.*	100–200	0.1–0.7	⋯	$\sim 6\times10^{-3}$	$\sim$6	0–2	⋯	⋯
This Letter	100–200	0.05–0.6	12 ± 2	10^{-3}–10^{-2}	0.5–2	0–2	0–1.5	0.01–0.8

tion of the relative speed of deformation $\dot{\delta}_k/v$, and we take v as proportional to the average speed of unloaded motors, i.e., $f(\dot{\delta}_k/v) = e^{-\dot{\delta}_k^2/v^2}$. In this way Eq. (2) leads to

$$\beta\gamma\dot{\delta}l + T_a e^{-\beta^2\delta l^2/v^2} + k\left(\beta + \frac{k_n}{2\alpha k}\right)\delta l = \frac{k_n}{2\alpha} l_0, \quad (3)$$

and the characteristic time associated with active contraction of axons is $\tau_{\mathrm{act}} \approx [1/(k\beta + \frac{k_n}{2\alpha})]\frac{T_a}{v}$.

From our experimental results in Fig. 4(a) and 4(b), we fit the values for T_a, v, and k using Eq. (3). In principle a fit to three parameters would seem excessive. However, the values obtained for T_a compare well to the initial tension T_0, differing in most cases by less than 30%. Since k is small, the equilibrium values of T_0 and T_a must be very close. Therefore, although T_a has been obtained from a fit of three parameters, it cannot be varied arbitrarily. Thus, our fit should allow us to estimate v and k with a reasonable precision. In addition, the values obtained for k, κ, and T_0 are compatible with those determined in previous works [8] (see Table I). However, the values of γ deduced here are somewhat smaller. A remarkable fact of these data is that T_a, and T_0 to a smaller degree, is correlated with v, showing a decreasing tendency with v. This could be a coincidence for the case of T_0 that can take any positive value smaller than T_a, but in our judgment it indicates that axons that contract faster exert smaller forces. This seems to be a natural consequence of the limited power of molecular motors. The axon power is of the order of $T_0 v \approx 24 \times 10^{-17}$ W for fast axons. In contrast, for characteristic speeds such that $v < 0.1$ μm/s, the axon tension T_0 is independent of v and the axon power increases linearly with v.

To conclude, we summarize the axon responses observed in our experiments. Figure 5 illustrates the connection between the passive and active behavior using the parameters defined in our model. Insets in Fig. 5 sketch the total response, T vs $\dot{\delta}_k$, when the viscous friction and motor effects are added together as both contributions are acting in parallel. For small T_a/v [Fig. 5, inset (i)], friction dominates and we observe a purely passive and monotonic case, in which the axon always elongates and, at final equilibrium, the motor tension component has to reach its final value near T_a by decreasing the elongation rate. Thus, the action of the molecular motors should influence the passive response of the axon at elongation rates that are positive but smaller than v. A similar behavior appears for moderate values of T_a/v, where the viscous response, γ, and molecular motors compete giving origin to an axon tension that is almost insensitive to $\dot{\delta}_k$, for small $\dot{\delta}_k$ [Fig. 5, inset (ii)]. For T_a/v relatively large, T vs $\dot{\delta}_k$ is dominated by the contribution of the molecular motors, producing a negative sensitivity to changes in $\dot{\delta}_k$ [Fig. 5, inset (iii)]. Then, the scenario for the transition from pure elongation to active contraction requires that, for decreasing viscous

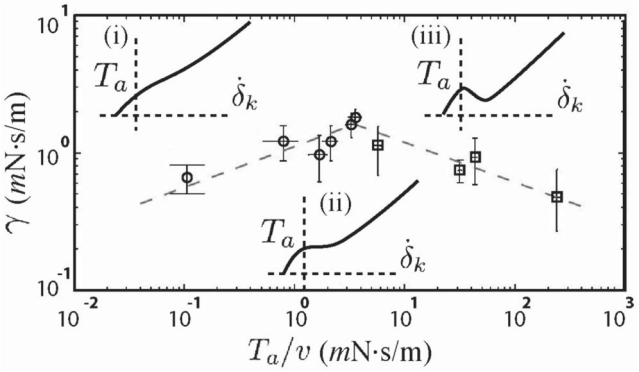

FIG. 5. Phase diagram defined by γ and T_a/v, passive (○) or active (□) behavior. Insets: active force plus viscous drag.

elongation ($\dot{\delta}_k > 0$), $\dot{\delta}_k$ must jump to negative rates of deformation in order to avoid the region of instability. Finally, similar to what occurs in the classic ''stick-slip'' type of problem, the ''relaxation'' observed here is a consequence of a force that decreases with increasing deformation speed [18]. In our case, viscous dissipation in competition with molecular motors determines under what general conditions negative elongation rate sensitivity exists.

This work was supported by Conicyt-Chile under program Fondap No. 11980002.

[1] B. Alberts *et al.*, *Molecular Biology of the Cell* (Garland Science, NY, 2002).
[2] A. K. Harris, P. Wild, and D. Stopak, Science **208**, 177 (1980).
[3] B. Fabry *et al.*, Phys. Rev. Lett. **87**, 148102 (2001).
[4] F. Wottawah *et al.*, Phys. Rev. Lett. **94**, 098103 (2005).
[5] P. Fernández, P. A. Pullarkat, and A. Ott, Biophys. J. **90**, 3796 (2006).
[6] F. J. Ahmad *et al.*, Nat. Cell Biol. **2**, 276 (2000).
[7] J. B. Phillips *et al.*, J. Physiol. **557**, 879 (2004).
[8] T. J. Dennerll *et al.*, J. Cell Biol. **109**, 3073 (1989).
[9] E. G. Banker and K. Goslin, *Culturing Nerve Cells* (MIT Press, Cambridge, MA, 1998).
[10] P. Lamoureux *et al.*, Nature (London) **340**, 159 (1989).
[11] T. J. Dennerll *et al.*, J. Cell Biol. **107**, 665 (1988).
[12] A proper expansion of the sine function gives an additional term for the nonlinear response in θ, $-(2T_0/3)\theta^3$, which is much smaller than $(\kappa L_x/2)\theta^3$ (see Table I).
[13] Yun-Bi *et al.*, Proc. Natl. Acad. Sci. U.S.A. **103**, 17 759 (2006).
[14] J. Howard, *Mechanics of Motor Proteins and the Cytoskeleton* (Sinauer, Sunderland, MA, 2001).
[15] K. Oiwa *et al.*, Proc. Natl. Acad. Sci. U.S.A. **87**, 7893 (1990), see Figs. 4 and 5.
[16] M. J. Schnitzer *et al.*, Nat. Cell Biol. **2**, 718 (2000).
[17] D. Riveline *et al.*, Eur. Biophys. J. **27**, 403 (1998).
[18] F. Jülicher and J. Prost, Phys. Rev. Lett. **75**, 2618 (1995).